



Adsorption Density Control of N719 on TiO₂ Electrodes for Highly Efficient Dye-Sensitized Solar Cells

Fumihiko Hirose,^{a,*} Koei Kuribayashi,^a Masaya Shikaku,^a Yuzuru Narita,^a
Yutaka Takahashi,^a Yasuo Kimura,^b and Michio Niwano^{b,*}

^aGraduate School of Science and Engineering, Yamagata University, Yamagata 992-8510, Japan

^bResearch Institute of Electrical Communication, Tohoku University, Sendai, 980-8577, Japan

N719 dye adsorption on anatase TiO₂ surfaces with different adsorption densities was investigated by IR-absorption spectroscopy using a multiple internal reflection technique. When the N719 dye was adsorbed on the TiO₂ surface by immersing it in an N719 solution consisting of acetonitrile and tertiary-butyl alcohol, chemisorbed and physisorbed N719 dyes coexisted on the surface. The ratio of chemisorbed and physisorbed dye densities was dependent on the N719 exposure, and excessive exposure led to the generation of the physisorbed dye. Test fabrications of the dye-sensitized solar cells (DSCs) with various N719 exposures suggested that we need to optimize the dye adsorption density to achieve a higher power conversion efficiency in DSCs.
© 2009 The Electrochemical Society. [DOI: 10.1149/1.3155425] All rights reserved.

Manuscript submitted January 26, 2009; revised manuscript received May 11, 2009. Published June 24, 2009.

Ever since O'Regan and Grätzel reported highly efficient, low cost dye-sensitized solar cells (DSCs) using *cis*-di(thiocyanato)bis(2,2'-bipyridyl-4,4''-dicarboxylate)ruthenium(II) (N719) with a photovoltaic efficiency of 11%,¹ many researchers have tried to reproduce the solar cell. Unfortunately, the attempts have all ended in failure as O'Regan and Grätzel did not release detailed information on the preparation of the TiO₂ electrode, which is the most important aspect of their innovation. Many papers have been published regarding TiO₂ fabrication to achieve larger surface areas for dye adsorption, in which nanoparticle TiO₂ films,¹⁻³ nanoparticle TiO₂ films mixed with relatively larger TiO₂ particles,⁴ particle TiO₂ with a high pore density,⁵ and TiO₂ nanotubes⁶ have been reported. As these surfaces with extremely large surface areas allowed for highly efficient power generation with a high density adsorption of the sensitizing dye, most researchers have been trying to achieve as high a density adsorption as possible. In a previous paper (see Ref. 7), however, the dye adsorbed on the TiO₂ surface consisted of chemisorbed and physisorbed dyes if dye adsorption was achieved by immersing the TiO₂ surface in the dye solution. Too much adsorption might limit power generation as the physisorbed dyes might prevent sunlight from reaching the chemisorbed dyes. However, the impact of physisorbed dyes on power generation has not, to date, been discussed.

Nazeeruddin et al. reported an investigation into N719 adsorption on TiO₂ nanoparticles using attenuated-total-reflection Fourier transform infrared absorption spectroscopy (IRAS).⁸ They proposed several adsorption models in which the N719 molecule anchors on the TiO₂ surface through one or two of its carboxyl groups. Leon et al. speculated on N719 anchors with a carboxylic moiety with a coordination of bridging or bidentate linkages.⁹ They found that the vibration frequency of COO⁻ changes, depending on whether the N719 is connected on the TiO₂ surface or physisorbed. These studies were helpful in understanding the adsorption mechanism of N719, although the discussion on the impact of physisorbed dyes was insufficient.

In this paper, we observed the adsorption states of the N719-sensitizing dye on anatase TiO₂ surfaces with a variety of adsorption densities using IRAS with a multiple-internal-reflection (MIR) geometry. Chemisorbed and physisorbed dyes coexisted on the dye-adsorbed surface. The ratio of the chemisorbed and the physisorbed dye densities was dependent on the exposure of the TiO₂ surfaces to the N719 dye, and overexposure generated a physisorbed state. Test fabrications of DSCs with various N719 exposures suggested that the degeneration of the physisorbed N719 is effective in enhancing

power generation. We discuss how to promote the power conversion efficiency of DSCs without interference of the physisorbed N719 dye in the photovoltaic operation.

Experimental

We investigated N719 adsorption by a TiO₂-coated GaAs prism using MIR-IRAS. The anatase TiO₂ was fabricated by metallorganic chemical vapor deposition (CVD) described elsewhere.^{10,11} The deposited TiO₂ had preferential orientations of (101), (200), and (211), which were confirmed by X-ray diffraction. The average thickness of the TiO₂ film was 0.1 μm, with an average roughness of less than 10 nm. The photocatalytic reaction of the deposited TiO₂ film was confirmed using MIR-IRAS, and the results were released elsewhere.¹² The chemical states of the sample surface before and after N719 adsorption were also monitored by MIR-IRAS. The experimental MIR-IRAS setup for the experiment in this paper is shown in Ref. 7. This technique was quite surface sensitive and had a higher resolution than other spectroscopic tools such as electron energy loss spectroscopy. The prism used for the MIR-IRAS measurements measured 0.5 × 10 × 40 mm, with 45° bevels on each of the short edges. IR radiation that exited an interferometer (Bomem MB-100) was focused at normal incidence onto one of the two bevels of the sample and propagated through a wafer, internally reflecting about 80 times.¹¹⁻¹⁵ The radiation that exited the other bevel of the sample was focused onto a liquid-N₂-cooled HgCdTe detector.

The N719 adsorption for the IRAS measurement was performed by dropping the N719 solution onto the TiO₂ surface. The N719 dye solution was a mixture of 10 mL acetonitrile and 10 mL tertiary-butyl alcohol containing N719 at a concentration of 0.36 mg/mL. When we dropped the dye onto the surface, we controlled the wet area so it was constant by the casting method. The wet surface was then air-dried at room temperature. The adsorption density of N719 was calculated by assuming that all N719 included in the dye solution remained uniformly on the surface.

In this study, we fabricated DSCs based on investigations made with MIR-IRAS. In the fabrication, TiO₂ films with a thickness of 56 μm with an area of 0.5 × 0.5 cm were formed on SnO₂-coated glass by drawing and extending TiO₂ paste using a glass rod and a plastic tape spacer. The TiO₂ paste was made from TiO₂ powder manufactured by Ishihara Sangyo (ST-01), deionized water, acetic acid solution with pH of 3.5, and poly(ethylene glycol). The TiO₂ films were baked in air at a temperature of 500°C for 1 h. The N719 adsorption was performed by dropping N719 solution onto the TiO₂ surface. The redox electrolyte was 0.1 M LiI, 0.05 M I₂, 0.6 M dimethyl propyl imidazolium iodide, and 0.5 M *tert*-butylpyridine in dried acetonitrile. The photovoltaic properties of the DSCs were measured using a current-voltage measurement system, and a 5000 K, 300 W xenon lamp was used as a light source. The light

* Electrochemical Society Active Member.

^z E-mail: fhirose@yz.yamagata-u.ac.jp

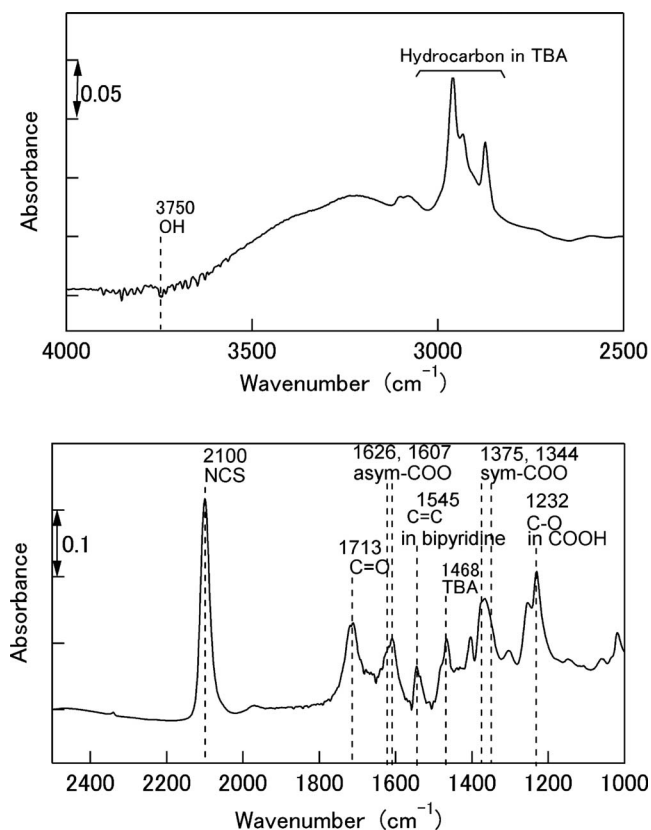


Figure 1. IR-absorption spectra obtained from a N719-adsorbed TiO₂ surface.

intensity at the DSC surface was set at 80 mW/cm² with a standard Si solar cell manufactured by Pecell Technologies.

Results and Discussion

The IR-absorption spectrum of the N719 dye adsorbed on TiO₂ is shown in Fig. 1. The N719 density on the TiO₂ surface was 3.8×10^{-3} mg/cm². The baseline for the calculation of the absorption spectrum is the IR transmission spectrum obtained from the TiO₂ film before N719 adsorption. In Fig. 1, the IR absorptions of hydrocarbon and NCS can be seen as 2800–3000 and 2100 cm⁻¹, respectively.^{8,9,12} The IR absorption by hydrocarbon was caused by tributylammonium (TBA) ions, which adsorbed to the surface during the course of the N719 adsorption. The IR absorption at 1468 cm⁻¹ can be ascribed to TBA counterions.⁹ Leon et al. also speculated that the TBA ions were separated from COOTBA in the dye solution to adsorb on the TiO₂ surface.⁹ The IR absorbance spectrum of symmetric vibration of the COO⁻ group can also be seen in Fig. 1. We can see double peaks in the spectrum. Leon et al. also reported that physisorbed N719 molecules such as N719 powder on its own exhibited IR absorption of COO at 1344 cm⁻¹, while chemically bonded N719 with bidentate or bridging linkage causes a shift to 1375 cm⁻¹.⁹ Some N719 molecules were chemisorbed to the TiO₂ surface and the others were isolated or physisorbed on the surface. The IR-absorption peak of COO asymmetric vibration mode at wavenumbers from 1606 to 1626 cm⁻¹ also consists of two chemical states of physisorbed and chemisorbed N719, which is discussed later. In Fig. 1, we can see a drop of absorbance at 3751 cm⁻¹, which indicates the degeneration of TiOH on the surface.⁷ This fact strongly suggests that the N719 dye adsorbs preferentially on OH sites on TiO₂ surfaces and makes bridges for electrons to the TiO₂ electrode with bidentate or bridging linkage. This explanation is supported by X-ray photoelectron spectroscopy studies released elsewhere.¹⁶ In a previous study,⁷ the intentional gen-

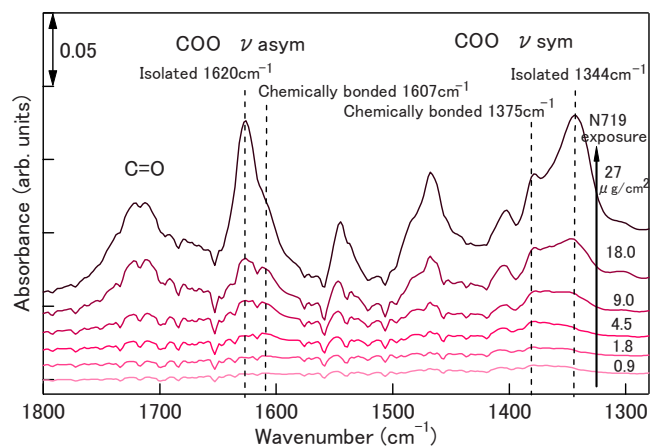


Figure 2. (Color online) Variation in IR-absorption spectra obtained from N719-adsorbed TiO₂ surfaces with various N719 exposures from 0.9 to 27 μg/cm². The dye was adsorbed on the surface by dropping a dye solution at various amounts and air drying the surface. The N719 dye solution was a mixture of 10 mL acetonitrile and 10 mL tertiary-butyl alcohol containing N719 at a concentration of 0.36 mg/mL.

eration of the OH sites on the TiO₂ electrodes with a photocatalytic reaction by UV irradiation in air before the N719 dye adsorption was effective in increasing the short-circuit current of the DSC, which is evidence of the above explanation.

In this work, we investigated variation in the chemical status of the bridging COO as a function of N719 dye exposure to discuss the impact of the physisorbed N719 dye on power generation in the DSCs. We show variations in IR-absorption spectra obtained from N719-adsorbed TiO₂ surfaces with various N719 exposures from 0.9 to 27 μg/cm² in Fig. 2. The dye was adsorbed on the surface by dropping a dye solution in various amounts and drying the surface. The N719 dye solution was a mixture of 10 mL acetonitrile and 10 mL tertiary-butyl alcohol containing N719 at a concentration of 0.36 mg/mL. The absorbance peaks of both COO symmetric and asymmetric vibration modes are modified by increasing the N719 exposure. In the symmetric vibration peak, the peak of physisorbed N719 at 1344 cm⁻¹ became prominent compared to the peak of the chemisorbed N719 at 1375 cm⁻¹.⁹ In the absorbance peak of the COO asymmetric vibration, the two states of 1620 and 1607 cm⁻¹ are confirmed, which are tentatively IR absorptions of COO of the physisorbed and chemisorbed N719. This assumption was supported by a simulation experiment using Gaussian. We calculated the vibration frequencies of simplified molecules of C₅H₅N-COOH and C₅H₅N-COO-TiX₃, which were used as simulation models for chemisorbed and physisorbed N719, respectively. X is heavy hydrogen with an atom mass of 10,000. The calculation was made with base functions of HF 6.31 gd. The energetically optimized structures of these molecules and simulated absorbance spectra are shown in Fig. 3. The wavenumber gap between COO symmetric and asymmetric vibrations becomes narrower when COOH becomes COO-TiX₃. This simulation suggests that the component of 1607 cm⁻¹ in the COO asymmetric vibration is due to the chemisorbed N719. In this simulation, the peak at 1750 cm⁻¹ appeared due to the change in the vibration frequency caused by the structural deformation of C-O. This suggests that monitoring of C-O vibration is also effective in discussing the adsorption status of the N719 dye, although we base our discussion only on the COO data, as the variation in the COO peak is clearer than that of C-O. The IRAS experiment in Fig. 2 suggests that excessive dye exposure leads to the coexistence of physisorbed and chemisorbed dyes on the TiO₂ surface, where physisorbed dyes may be stacked on the chemisorbed dyes on the TiO₂ surface. We should optimize dye exposure as excessive exposure led to the enhancement of the physisorbed N719 dye, which would deteriorate the power conversion efficiency of

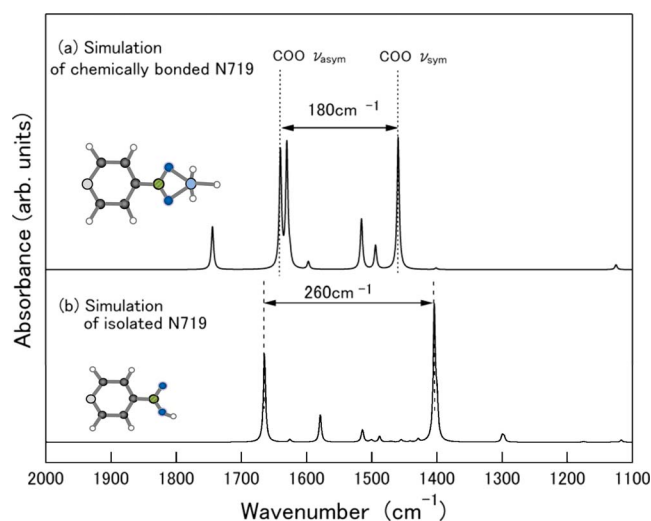


Figure 3. (Color online) Simulations of COO asymmetric and symmetric vibrations of chemically bonded and physisorbed N719. Simplified molecules of $C_5H_5N-COOH$ and $C_5H_5N-COO-TiX_3$ were used as simulation models for chemically bonded and physisorbed N719, respectively. X is a heavy hydrogen atom with an atom mass of 10,000.

DSC as described below. For the current CVD-grown TiO_2 , the optimized exposure was expected from around 4.5 to $9 \mu g/cm^2$, although the optimized exposure is greatly increased for the porous nanoparticle TiO_2 films for DSCs as shown later.

To investigate the availability of optimization of N719 exposure in DSCs, we fabricated DSCs using various dye exposures. Figure 4 shows the variation in the power conversion efficiency of DSCs with various N719 exposures. In this experiment, a 5000 K, 300 W xenon lamp was used as a light source. The light intensity was 80 mW/cm^2 . The power conversion efficiency increased from 0.01 mg/cm^2 and reached its maximum at 0.7 mg/cm^2 . Too much exposures from this point resulted in a deterioration of power generation in the DSCs. Figure 5 shows the power generation characteristics measured from the samples made by immersing the surface in the dye solution and by exposing the surface to the N719 solution with a density of 0.7 mg/cm^2 . The short-circuit current density of J_{sc} was improved from 6.77 to 7.14 mA/cm^2 . The power conversion efficiency was also improved from 4.56 to 4.78% . In this experiment, we fabricated 10 samples for each state. The standard deviation of the power conversion efficiency was as low as 0.15% . The obtained power generation data are summarized in Table I. The result indicates that the elimination of the physisorbed N719 dye enhances power generation. The open-circuit voltage was decreased by

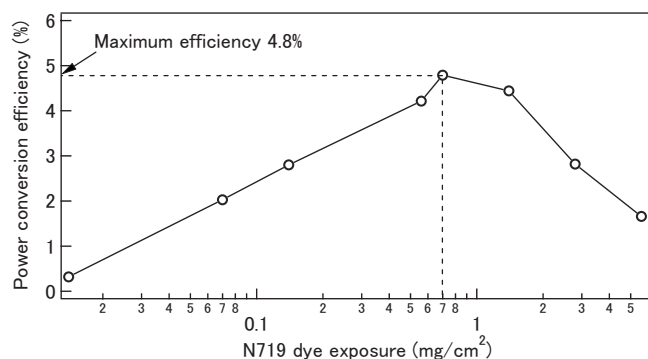


Figure 4. Variation in power conversion efficiency of DSCs with various N719 exposures. In this experiment, a 5000 K, 300 W xenon lamp was used as a light source. The light intensity was 80 mW/cm^2 .

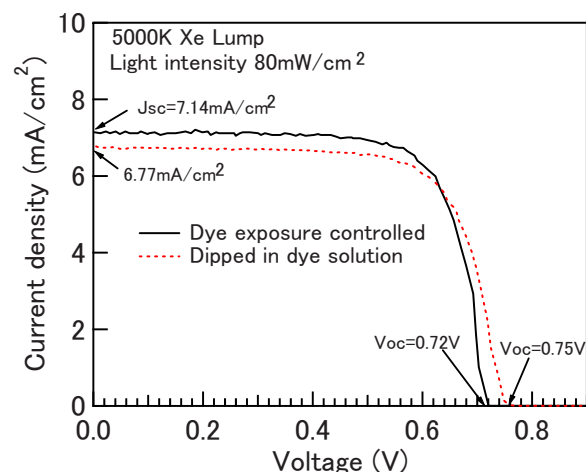


Figure 5. (Color online) Power generation characteristics measured from samples obtained by immersing the samples in a dye solution and dropping the N719 solution onto the sample surface with a density of 0.7 mg/cm^2 .

controlling the adsorption density. The physisorbed dye plays the role of inhibiting the carrier recombination of electron and hole between bare TiO_2 electrode and electrolyte, as the physisorbed dye may block I_3^- ions from reaching the bare TiO_2 to reduce them, although further investigation is necessary to prove the assumption. The DSC fabrication experiment supports the ability of N719 exposure control to eliminate the interference of the physisorbed N719.

Here the difference of the optimized exposure between the CVD-grown and nanoparticle TiO_2 surfaces was noted. As can be seen in Ref. 1-6, nanoparticle TiO_2 has larger surface areas compared to the CVD-grown flat TiO_2 . Tsoukleris et al. reported that a nanoporous TiO_2 electrode made with 2-ethyl-1-hexanol-based TiO_2 paste has roughness factors from 440 to 550.¹⁷ If we assume the roughness factor of our nanoporous TiO_2 electrode as 500, the optimized N719 exposure for the nanoporous TiO_2 estimated by the IRAS experiment is calculated in the range $2.25-4.5 \text{ mg/cm}^2$. The gap between the estimation and experiment is due to the difference of surface crystal orientation.

In this paper, we demonstrated a method to eliminate the physisorbed N719 dye in the adsorption by controlling its exposure. Other possible methods to suppress the physisorbed N719 are discussed below. In our previous work, intentional hydroxylation by a photocatalytic reaction on the TiO_2 surface is effective in increasing the density of the adsorbed N719 selectively.⁷ Some researchers have reported a dye-adsorption method whereby the TiO_2 surface is immersed in the dye solution, followed by rinsing it in ethanol.¹⁶ We can expect an effect of eliminating the physisorbed dye during the rinse process, although in our experience, the chemisorbed dye was in fact removed from the surface during the rinse process. As another method, we are considering changing the dye solution temperature at dye adsorption as the ratio of physisorbed and chemisorbed dyes must be determined by the equilibrium of the adsorption and desorption reactions. In our investigation, decreasing or increas-

Table I. Power generation data measured from samples obtained (A) by immersing the sample in the dye solution and (B) by dropping the N719 solution onto the sample surface with a density of 0.7 mg/cm^2 . The light exposure for power generation was 80 mW/cm^2 . FF is fill factor.

Sample	J_{sc} ($\text{cm}^2/\text{V s}$)	V_{oc} (V)	FF	Efficiency (%)
(A) Conventional method	6.77	0.75	0.72	4.56
(B) Optimized exposure	7.14	0.72	0.74	4.78

ing the solution temperature from room temperature enhanced the generation of the chemisorbed dye. The results are discussed elsewhere.

Conclusions

The adsorption state of N719-sensitizing dye on anatase TiO₂ surfaces with a variety of adsorption densities was investigated using MIR-IRAS. When the N719 dye was adsorbed on the anatase TiO₂ surface by exposing it in a N719 solution made with acetonitrile and tertiary-butyl alcohol, chemisorbed and physisorbed N719 dyes coexisted on the surface. The ratio of chemisorbed and physisorbed dye densities was dependent on the dye exposure, and excessive exposure led to the enhancement of physisorbed N719. We need to optimize the dye adsorption density to achieve higher efficiencies in DSCs. This study provides an in-depth insight into achieving low cost, high performance DSCs.

Yamagata University assisted in meeting the publication costs of this article.

References

1. B. O'Regan and M. Grätzel, *Nature (London)*, **353**, 737 (1991).
2. J. Jiu, S. Isoda, M. Adachi, and F. Wang, *J. Photochem. Photobiol., A*, **189**, 314 (2007).
3. T. V. Nguyen, H. C. Lee, and O. Yang, *Sol. Energy Mater. Sol. Cells*, **90**, 967 (2006).
4. Z. Wang, H. Kawauchi, T. Kashima, and H. Arakawa, *Coord. Chem. Rev.*, **248**, 1381 (2004).
5. Y. Saito, S. Kanbe, T. Kitamura, Y. Wada, and S. Yanagida, *Sol. Energy Mater. Sol. Cells*, **83**, 1 (2004).
6. S. Uchida, R. Chiba, M. Tomiha, N. Masaki, and M. Shirai, *Nanotechnology in Messtructured Materials*, **146**, 791 (2003).
7. F. Hirose, K. Kuribayashi, T. Suzuki, Y. Narita, Y. Kimura, and M. Niwano, *Electrochem. Solid-State Lett.*, **11**, A109 (2008).
8. M. K. Nazeeruddin, R. Humphry-Baker, P. Liska, and M. Grätzel, *J. Phys. Chem. B*, **107**, 8981 (2003).
9. C. P. Leon, L. Kador, B. Peng, and M. Thelakkat, *J. Phys. Chem. B*, **110**, 8723 (2006).
10. S. Tokita and N. Tanaka, *Jpn. J. Appl. Phys., Part 1*, **39**, 169 (2000).
11. F. Hirose, M. Ito, and K. Kurita, *Jpn. J. Appl. Phys.*, **47**, 5619 (2008).
12. F. Hirose, M. Kurita, Y. Kimura, and M. Niwano, *Appl. Surf. Sci.*, **253**, 1912 (2006).
13. M. Niwano, M. Terashi, and J. Kuge, *Surf. Sci.*, **420**, 6 (1999).
14. M. Shinohara, Y. Kimura, M. Saito, and M. Niwano, *Surf. Sci.*, **502**, 96 (2002).
15. M. Shinohara, M. Niwano, Y. Neo, and K. Yakoo, *Thin Solid Films*, **369**, 16 (2000).
16. E. M. Johansson, M. Hedund, H. Siegbahn, and H. Rensmo, *J. Phys. Chem. B*, **109**, 22256 (2005).
17. D. S. Tsoukleris, I. M. Arabatzis, E. Chatzivasiloglou, A. I. Kontos, V. Belese, M. C. Bernard, and P. Falaras, *Sol. Energy*, **79**, 422 (2005).